

Axial-vector dominance predictions in quasielastic neutrino-nucleus scattering

J. E. Amaro, E. Ruiz Arriola

*Departamento de Física Atómica, Molecular y Nuclear and Instituto Carlos I de Física Teórica y Computacional,
Universidad de Granada, E-18071 Granada, Spain*

Abstract

We use the minimum meson-dominance ansatz compatible with low- and high energy constraints to model the nucleon axial form factor. The parameters of the resulting axial form factor are the masses and widths of the two axial mesons, incorporated as a product of monopoles. By applying the half width rule in a Monte Carlo simulation a distribution of theoretical predictions can be generated for the neutrino-nucleus quasielastic cross section. We test the model by applying it to the (ν_μ, μ) quasielastic cross section from ^{12}C for the kinematics of the MiniBooNE experiment. The resulting predictions have no free parameters. The relativistic Fermi gas model globally reproduces the experimental data, giving $\chi^2/\text{\#bins} = 0.81$. A Q^2 dependent error analysis of the neutrino data shows that the uncertainties in the axial form factor $G_A(Q^2)$ are comparable to the ones induced by the a priori half width rule.

1. Introduction

Since the first measurement of the muon neutrino charged current quasielastic double differential cross section [1, 2, 3] many attempts have been made to characterize an effective axial-vector form factor of the nucleon [4, 5, 6, 7]. This is often made in terms of an dipolar axial mass M_A , assuming a dipole form $G_A(Q^2) = g_A/(1 - Q^2/M_A^2)^2$ [8, 9], for $Q^2 < 0$. The world average value of the nucleon dipolar axial mass is $M_A \sim 1$ GeV [10]. The MiniBooNE cross section data are too large compared to the theoretical models of quasielastic neutrino scattering in the impulse approximation, unless a significant larger value of $M_A \sim 1.35$ GeV is employed in the nuclear axial current. Microscopic explanations of the large value of M_A have been proposed based on ingredients involving multinucleon emission, short range correlations and meson exchange currents [11, 12, 8]. Recently studies with a monopole parametrization have been performed in [13] as well as nucleon mean field effective mass analyses of blurred electron scattering data [14]. The disparate values obtained upon consideration of different nuclear effects can be regarded as a genuine systematic errors. Those turn out to be much larger than the alleged statistical uncertainties which would lead to the most precise determination of the axial form factor to date in the range $|Q^2| \lesssim 2\text{GeV}^2$. A careful statistical analysis has been undertaken more recently [15] and some tension among different data in different models has been reported.

Despite the phenomenological success, the dipole form factor while enjoys the pQCD result [17] asymptotically, $G_A \sim 1/Q^4$, finds no further theoretical support at finite Q^2 . Moreover, a one parameter fit introduces a bias linking high and low

energies unnaturally. To overcome this problem a model independent analysis of axial form factor using dispersion relations under definite convergence assumptions and based on neutrino scattering was performed [18], with the finding that errors of a dipole ansatz may be underestimated. To be fair one should say that the neutrino scattering vs nucleon axial form factor is a kind of red herring. A duality based parameterization has been proposed [19]. Since neutrino based determinations often imply certain and questionable assumptions, it is instructive to review other sources of information.

The first lattice QCD determination of the axial form factor [20] provided $M_A = 1.03(5)\text{GeV}$ in agreement with world average neutrino data at the time $M_A = 1.032(36)\text{GeV}$. However, subsequent calculations [21] yield $M_A = 1.5\text{GeV}$, a number which has recently been confirmed [22] for unphysical pion masses (about twice the physical value); the corresponding dipolar axial mass is larger than the experimental one, although there is some trend to agreement as the pion mass approaches the physical value. The role of excited states has been analyzed in a more recent lattice analysis [23] confirming these results. In addition, Light cone QCD sum rules also overestimate the experimental dipole fit by 30% [24] in the range $1 < |Q^2| < 4\text{GeV}^2$, a trend checked by subsequent analyses [25, 26] and agreeing also with lattice calculations.

On the more phenomenological hadronic level, the algebra of fields [27] which yields field-current identities [28] imply a generalized meson dominance which has proven as a convenient tool to analyze many important hadronic properties and most notably generalized vertex functions and hadronic form factors [29]. In the particular case of conserved currents, and more specifically axial-vector currents the general form of the form factor is expected to be a sum of infinitely many monopoles with isovector *axial* meson masses, whereas the pQCD result [17] yields $G_A \sim 1/Q^4$. The goodness of

Email addresses: amaro@ugr.es (J. E. Amaro), earriola@ugr.es (E. Ruiz Arriola)

AV-dominance for the axial nucleon form factor was posed in Ref.[30] by including the strong vertex corrections. However, meson dominance implies exchange of resonances which have a mass spectrum characterized by a mass and a width. Amazingly there is a theoretical limit where meson-dominance with narrow resonances becomes true in QCD, namely the large N_c -limit introduced by 'tHooft and Witten long ago [31, 32]; within the large N_c expansion mesons become stable particles. Their width-to-mass ratio is $\Gamma_R/M_R = \mathcal{O}(1/N_c) \sim 0.33$ which turns out to give the correct order of magnitude of the average experimental value 0.12(8) [33]. The phenomenological implications of meson dominance within a large N_c approach have been analyzed in Ref. [16] and after natural uncertainty estimates based on the resonance width good description of data and lattice was achieved.

Motivated by these theoretical insights, in the present paper we explore the N_c -based parametrization of the nucleon axial form factor [16]. While some authors claim that, after including the relevant nuclear and reaction mechanisms, the Mini-BooNE data are fully compatible with former determinations of the nucleon dipolar axial mass [8], the fact is that the dipole approximation cannot be justified from a field-theoretic point of view and is in contradiction with quark-hadron duality at large N_c [16]. Instead, in the present work we explore the consequences of axial-vector dominance directly to neutrino scattering by combining it with the relativistic Fermi gas. We do this without fitting any neutrino data. This allows to address clearly some important issues from a statistical point of view.

2. Axial-vector dominance and the axial form factor

Axial-Vector dominance was first introduced by Lee and Zumino [28] into particle physics as a very natural generalization of the successful realization that Vector-Meson dominance. It simply states that the axial-vector current is given by the current field identity, which for just u, d quarks reads

$$J_A^\mu(x) = \frac{1}{2} \bar{q} \gamma_\mu \gamma_5 \vec{\tau} q = \sum_A f_A \vec{A}_\mu(x) + \sum_P f_P \partial_\mu \vec{P}(x) \quad (1)$$

where f_A and f_P are the decay amplitudes of the axial-vector $A = a_1, a'_1, \dots$ and pseudoscalar mesons $P = \pi, \pi', \dots$ respectively. This equation yields a generalized PCAC, which implies in turn a generalization of the Goldberger-Treiman relation [34].

As a consequence the axial form factor of the nucleon can be written as a sum of monopole form factors. As noted in Ref. [16] one of the problems with this identity is that generally the interpolating fields are resonances which have a mass and a width, and we stand by the solution proposed there to use the width as a genuine uncertainty of the meson dominance ansatz. Likewise, in this paper we use the minimal ansatz for axial nucleon form factor furnishing meson dominance and proper pQCD behavior

$$G_A(Q^2) = g_A \frac{m_{a_1} m_{a'_1}}{(m_{a_1}^2 - Q^2)(m_{a'_1}^2 - Q^2)} \quad (2)$$

with $g_A = 1.26$, and where the axial meson masses are $m_{a_1} = 1.230$ GeV, $m_{a'_1} = 1.647$ GeV. The experimental widths are $\Gamma_{a_1} = 0.425$ GeV, and $\Gamma_{a'_1} = 0.254$ GeV as listed in the PDG compilation [35]¹. The masses are only the central values of the axial mesons spectra. We use the half-width rule to generate random values for m_{a_1} and $m_{a'_1}$ following Gaussian distributions with variances $\Gamma_{a_1}/2$ and $\Gamma_{a'_1}/2$ respectively. This provides a distribution band for the axial form factor [16] which is above the data but agrees well with the lattice [21, 22, 23] and light cone QCD sum rules estimates [24, 25, 26]. These are general features of the meson dominated form factors also for electromagnetic, scalar and gravitational form factors. We will thus apply this axial form factor band for the neutrino cross section theoretical predictions. Our view point is that given the many effects which might contribute to neutrino-nucleus scattering it may be sensible to use a credible form factor with an error estimate based on a different source of data, without resting on a specific fit to the neutrino data.

After presenting our main results we will also analyze this fitting possibility for completeness. We want to investigate the traditional point of view of *assuming* certain nuclear effects before undertaking a fit of the axial form factor of the nucleon. For example in Ref. [8] the inclusion of several effects such as RPA correlations and MEC have been considered and a fit to the axial form factor has been undertaken assuming a fixed $\Delta - N$ -transition form factor. We want to understand why in these studies one can extract more accurate information on the axial form factor than on the nuclear model response functions.

3. Quasielastic neutrino scattering

In this paper we are interested in the charged-current quasielastic (CCQE) reactions in nuclei induced by neutrinos. In particular we compute the (ν_μ, μ^-) cross section. The total energies of the incident neutrino and detected muon are $\epsilon = E_\nu$, $\epsilon' = m_\mu + T_\mu$, and their momenta are \mathbf{k}, \mathbf{k}' . The four-momentum transfer is $Q^\mu = k^\mu - k'^\mu = (\omega, \mathbf{q})$, with $Q^2 = \omega^2 - q^2 < 0$. If the lepton scattering angle is θ , the double-differential cross section can be written as [36, 37]

$$\frac{d^2\sigma}{dT_\mu d\cos\theta}(E_\nu) = \left(\frac{M_W^2}{M_W^2 - Q^2} \right)^2 \frac{G^2 \cos^2 \theta_c}{4\pi} \frac{k'}{\epsilon} v_0 S_\pm \quad (3)$$

Here $G = 1.166 \times 10^{-11} \text{ MeV}^{-2} \sim 10^{-5}/m_p^2$ is the Fermi constant, θ_c is the Cabibbo angle, $\cos \theta_c = 0.975$, and the kinematic factor $v_0 = (\epsilon + \epsilon')^2 - q^2$.

The nuclear structure function S_\pm is defined as a linear combination of the five nuclear response functions (+ is for neutrinos and - is for antineutrinos)

$$S_\pm = V_{CC} R_{CC} + 2V_{CL} R_{CL} + V_{LL} R_{LL} + V_T R_T \pm 2V_{T'} R_{T'}, \quad (4)$$

¹Of course this ansatz provides a value for the msr axial radius, $\langle r^2 \rangle_A = 6/m_{a_1}^2 + 6/m_{a'_1}^2$. One can add a further axial state fixing the radius to its precise value, and comply to the pQCD short distance constraint but the effect is not large. This way one might take into account, the tiny and predictable differences between axial radii determined by either electroproduction or neutrino scattering.

where the V_K coefficients depends only on the neutrino and muon kinematics and do not depend on the details of the nuclear target.

$$V_{CC} = 1 - \delta^2 \frac{|Q^2|}{v_0} \quad (5)$$

$$V_{CL} = \frac{\omega}{q} + \frac{\delta^2 |Q^2|}{\rho' v_0} \quad (6)$$

$$V_{LL} = \frac{\omega^2}{q^2} + \left(1 + \frac{2\omega}{q\rho'} + \rho\delta^2\right) \delta^2 \frac{|Q^2|}{v_0} \quad (7)$$

$$V_T = \frac{|Q^2|}{v_0} + \frac{\rho}{2} - \frac{\delta^2}{\rho'} \left(\frac{\omega}{q} + \frac{1}{2}\rho\rho'\delta^2\right) \frac{|Q^2|}{v_0} \quad (8)$$

$$V_{T'} = \frac{1}{\rho'} \left(1 - \frac{\omega\rho'}{q}\delta^2\right) \frac{|Q^2|}{v_0}. \quad (9)$$

where we have defined the adimensional factors $\delta = m' / \sqrt{|Q^2|}$, proportional to the muon mass m' , $\rho = |Q^2|/q^2$, and $\rho' = q/(\epsilon + \epsilon')$.

We evaluate the five nuclear response functions R_K , $K = CC, CL, LL, T, T'$ (C =Coulomb, L =longitudinal, T =transverse). following the simplest approach that treats exactly relativity, gauge invariance and translational invariance, that is the relativistic Fermi gas model (RFG) [36, 37]. The single nucleons are described by plane wave spinors and the response functions are analytical. It is a remarkable result that the nuclear response function R_K of the RFG is proportional to a single-nucleon response function U_K times the so-called scaling function $f(\psi)$

$$R_K = \frac{N\xi_F}{m_N\eta_F^3 K} U_K f(\psi) \quad (10)$$

where N is the neutron number, $\eta_F = k_F/m_N$, and $\xi_F = \sqrt{1 + \eta_F^2} - 1$. The scaling function is defined as

$$f(\psi) = \frac{3}{4}(1 - \psi^2)\theta(1 - \psi^2) \quad (11)$$

where θ is the Heavyside step function and ψ is the scaling variable

$$\psi^2 = \frac{1}{\xi_F} \max \left\{ \kappa \sqrt{1 + \frac{1}{\tau}} - \lambda - 1, \xi_F - 2\lambda \right\} \quad (12)$$

where $\lambda = \omega/(2m_N)$, $\kappa = q/(2m_N)$, and $\tau = \kappa^2 - \lambda^2$.

Finally, we give the single-nucleon responses U_K . For $K = CC$ it is the sum of vector and axial-vector response, in turns written as the sum of conserved (c.) plus non conserved (n.c.) parts,

$$U_{CC} = U_{CC}^V + (U_{CC}^A)_c + (U_{CC}^A)_{n.c.} \quad (13)$$

For the vector CC response we have

$$U_{CC}^V = \frac{\kappa^2}{\tau} \left[(2G_E^V)^2 + \frac{(2G_M^V)^2 + \tau(2G_M^V)^2}{1 + \tau} \Delta \right], \quad (14)$$

where G_E^V and G_M^V are the isovector electric and magnetic nucleon form factors (we use Galster's parametrization), and

$$\Delta = \frac{\tau}{\kappa^2} \xi_F (1 - \psi^2) \left[\kappa \sqrt{1 + \frac{1}{\tau}} + \frac{\xi_F}{3} (1 - \psi^2) \right]. \quad (15)$$

The axial-vector CC response is the sum of conserved (c.) plus non conserved (n.c.) parts,

$$(U_{CC}^A)_c = \frac{\kappa^2}{\tau} G_A^2 \Delta \quad (16)$$

$$(U_{CC}^A)_{n.c.} = \frac{\lambda^2}{\tau} (G_A - \tau G_P)^2. \quad (17)$$

where G_A is the nucleon axial-vector form factor and G_P the pseudoscalar axial form factor. From PCAC the pseudoscalar form factor is

$$G_P = \frac{4m_N^2}{m_\pi^2 - Q^2} G_A. \quad (18)$$

Similarly, for $K = CL, LL$ we have

$$U_{CL} = U_{CL}^V + (U_{CL}^A)_c + (U_{CL}^A)_{n.c.} \quad (19)$$

$$U_{LL} = U_{LL}^V + (U_{LL}^A)_c + (U_{LL}^A)_{n.c.}, \quad (20)$$

The vector and conserved axial-vector parts are determined by current conservation

$$U_{CL}^V = -\frac{\lambda}{\kappa} U_{CC}^V \quad (21)$$

$$(U_{CL}^A)_c = -\frac{\lambda}{\kappa} (U_{CC}^A)_c. \quad (22)$$

$$U_{LL}^V = \frac{\lambda^2}{\kappa^2} U_{CC}^V \quad (23)$$

$$(U_{LL}^A)_c = \frac{\lambda^2}{\kappa^2} (U_{CC}^A)_c, \quad (24)$$

while the n.c. parts are

$$(U_{CL}^A)_{n.c.} = -\frac{\lambda\kappa}{\tau} (G_A - \tau G_P)^2 \quad (25)$$

$$(U_{LL}^A)_{n.c.} = \frac{\kappa^2}{\tau} (G_A - \tau G_P)^2. \quad (26)$$

Finally the transverse responses are given by

$$U_T = U_T^V + U_T^A \quad (27)$$

$$U_T^V = 2\tau(2G_M^V)^2 + \frac{(2G_E^V)^2 + \tau(2G_M^V)^2}{1 + \tau} \Delta \quad (28)$$

$$U_T^A = 2(1 + \tau)G_A^2 + G_A^2 \Delta \quad (29)$$

$$U_{T'} = 2G_A(2G_M^V) \sqrt{\tau(1 + \tau)} [1 + \tilde{\Delta}] \quad (30)$$

with

$$\tilde{\Delta} = \sqrt{\frac{\tau}{1 + \tau}} \frac{\xi_F(1 - \psi^2)}{2\kappa}. \quad (31)$$

4. Numerical results

In Fig.1 we show the meson-dominance predictions for the total integrated CCQE cross section

$$\sigma(E_\nu) = \int dT_\mu \int d\cos\theta \frac{d^2\sigma}{dT_\mu d\cos\theta}(E_\nu). \quad (32)$$

The theoretical uncertainties represented by the displayed band have been computed by a Monte carlo calculation assuming a

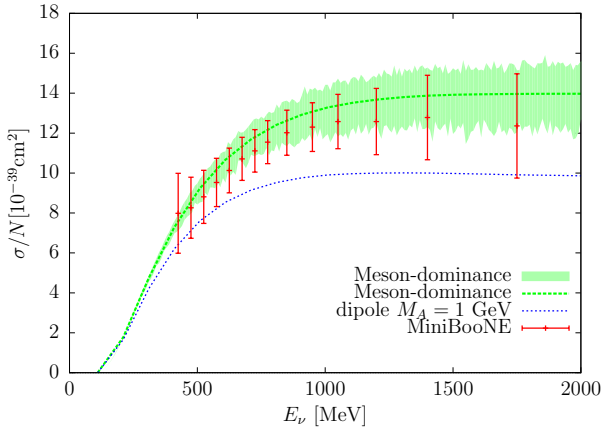


Figure 1: Integrated quasielastic neutrino cross section of ^{12}C . The axial meson dominance band prediction is centered around the axial meson masses, and it is compared to the dipole parametrization with dipolar axial mass $M_A = 1$ GeV. The experimental data are from MiniBooNE experiment.

Gaussian distribution for the axial meson mass distributions. For comparison we show also the results obtained with a dipole axial form factor with $M_A = 1$ GeV. The MiniBooNE data are compatible with the axial meson-dominance predictions. Note that no attempts to fit the experimental data have been made. The only parameter of the RFG model is the Fermi momentum $k_F = 225$ MeV.

The MiniBooNE unfolded energy dependent cross section is model dependent based on a reconstruction of the neutrino energies assuming a quasielastic interaction with a neutron at rest. These data suffer from uncertainties driven by the model dependence of the neutrino energy reconstruction. For proper and useful comparisons, the flux-averaged doubly differential cross section should be used. We compute this cross section as

$$\frac{d^2\sigma}{dT_\mu d\cos\theta} = \frac{\int dE_\nu \phi(E_\nu) \frac{d^2\sigma}{dT_\mu d\cos\theta}(E_\nu)}{\int dE_\nu \phi(E_\nu)} \quad (33)$$

where $\phi(E_\mu)$ is the incident neutrino flux.

In figure 2 we show results for the flux-averaged doubly differential CCQE cross section as a function of the muon kinetic energy. The bands are the axial meson-dominance model predictions for fixed values of $\cos\theta$ at the center of the experimental bins.

The MiniBooNE ν_μ CCQE flux-integrated double differential cross section is provided in bins (t_i, t_{i+1}) of T_μ and bins (c_j, c_{j+1}) of $\cos\theta$. The size of the bins is $c_{j+1} - c_j = \Delta c = \Delta \cos\theta_\mu = 0.1$, and $t_{i+1} - t_i = \Delta t = \Delta T_\mu = 0.1$ GeV.

For a meaningful comparison with the experimental data we have computed the averaged cross section for each bin, by integrating the doubly-differential cross section over each discrete bin.

$$\Sigma_{ij} = \frac{1}{\Delta t \Delta c} \int_{t_i}^{t_{i+1}} dT_\mu \int_{c_j}^{c_{j+1}} d\cos\theta \frac{d^2\sigma}{dT_\mu d\cos\theta}. \quad (34)$$

The axial vector dominance predictions for the averaged cross section Σ_{ij} are also shown in figure 2, where they are

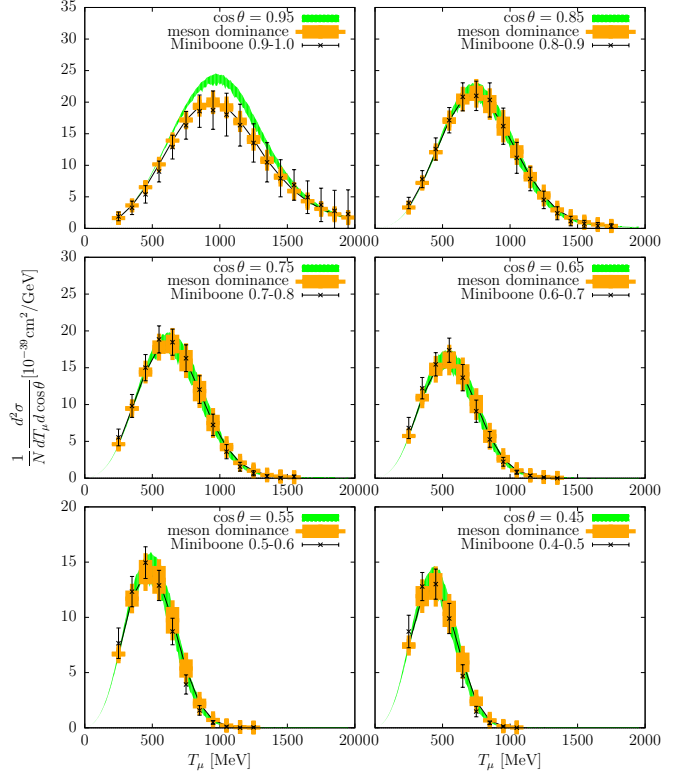


Figure 2: Flux-averaged doubly differential CCQE cross section as a function of the muon kinetic energy. The continuous band predictions (green) have been computed for fixed values of $\cos\theta$ at the center of the experimental bins. The discrete meson dominance predictions have been computed by integrating the doubly-differential cross section over each discrete bin.

compared to the experimental data. The theoretical errors are again computed by assuming a Gaussian distribution of the axial meson masses. Note that the averaged cross section for low scattering angles, bin $\cos\theta = 0.9-1.0$, is quite different from the cross section at the central value $\cos\theta = 0.95$. This is due to the strong angular dependence of the differential cross section for small angles, as can be seen in Fig. 3. Therefore the integration of the cross section over the bin is crucial to get the correct average. Note also that in this region the momentum transfer takes the smallest values compatible with energy transfer, and one expects that the model dependence of the results be maximized. As a matter of fact according to Ref. [38] the shell structure effects for both discrete and continuum are essentially washed out in favor of the RFG. For larger scattering angles, the angular dependence is mild, and the value of the cross section at the center of the bin is closer to the average, Eq. (34), as can be seen in Fig. 2.

5. Goodness of the model

To get a global measure of the goodness of the model in describing the experimental data, we compute the distance of the theory to data as given by a χ^2 metric, defined as $\chi^2 = \sum_{i,j} \chi_{ij}^2$. The χ_{ij} matrix provides the distance between theory and experiment within each bin (i, j) , in units of the total uncertainty. It

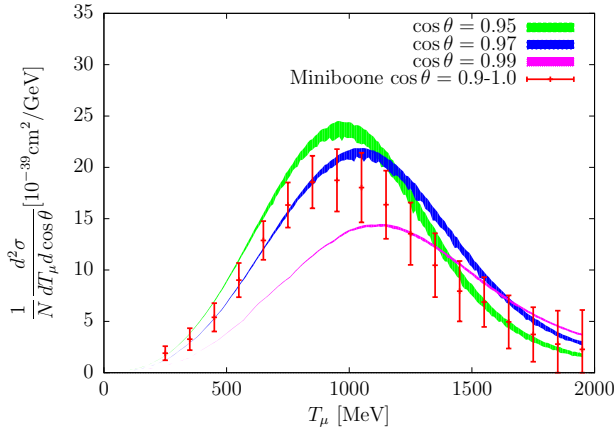


Figure 3: Flux-averaged doubly differential CCQE cross section for several values of $\cos \theta$, and for low scattering angles, compared with the experimental data for the bin $\cos \theta = 0.9-1.0$.

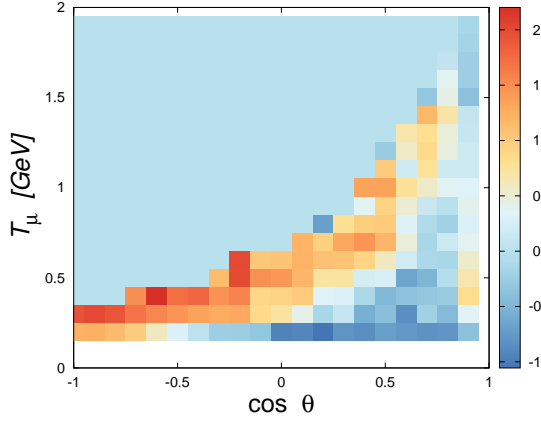


Figure 4: The χ_{ij} computed values for each bin pair are represented in the $(\cos \theta_\mu, T_\mu)$ plane as a color image.

is defined as

$$\chi_{ij} = \frac{\Sigma_{ij}^{(th)} - \Sigma_{ij}^{(exp)}}{\sqrt{(\Delta \Sigma_{ij}^{(th)})^2 + (\Delta \Sigma_{ij}^{(exp)})^2}} \quad (35)$$

where $\Delta \Sigma_{ij}^{(exp)}$ is the experimental error. and $\Delta \Sigma_{ij}^{(th)}$ is the theoretical uncertainty due to the physical widths of the axial mesons. In Fig. 4 we show the matrix values χ_{ij} computed for all the bins of the MiniBooNE CCQE neutrino experiment. We obtain $\chi^2 = 111$, so that dividing by the number of bins $N = 137$, we get $\chi^2/N = 0.81$. The model agrees remarkably well with data taking into account that we don't minimize χ^2 and we just compute it.

While the χ^2 value seems to be acceptable, let us analyze the assumptions underlying the comparison. We are just testing that the difference between the theory and the data should behave as a random variable, namely a standardized normal distribution. However, a look to the Fig. 4 reveals that the level of disagreement is located at the edges of the plot, while we should expect a more uniform pattern. This can be further elucidated by ana-

lyzing the differences. We find that there is a strong asymmetry in the residuals, indicating gross systematic differences. Thus, we believe that these large discrepancies are possibly beyond the applicability of the RFG. At the same time one should also admit that the double binning procedures tend to wash out nuclear effects.

Some fits to the dipolar axial mass do generate rather good χ^2 values and unprecedented accuracy for the axial form factor. Let us remind that, a too low value is as bad as a too high value, since the χ^2 -distribution for a large number of degrees of freedom $\nu = N - P$ behaves as a Gaussian distribution and thus it must be $\chi^2/\nu = 1 \pm \sqrt{2/\nu}$ within 1σ confidence level. For instance in Ref. [8] a value of $\chi^2/\nu = 33/(137 - 2) = 0.24$ was obtained which is outside the expected confidence level by 6σ . This suggest that experimental errors may be too large, and the question is whether errors can be reduced without destroying the Gaussian nature of the fluctuations. Moreover, the statistical approach deals with testing the validity of a given functional form for the *true* form factor, while despite the much extended practice there is no theoretical support for a dipole form factor.

In order to understand those results we have performed a conventional χ^2 -fit with two axial masses as minimization parameters. For this fit we include only the experimental errors in the denominator of Eq. (35). As in Ref. [8] we normalize the data by a factor $\lambda = 0.96$ and subtract a constant Q -value $Q_b = 17$ MeV to the energies of the particle-hole excitations (note that while this modification by hand of the RFG energies improves the fit, the gauge invariance of the model is broken). We find the minimum at $m_{a_1} = m_{a'_1} = 1293$ with $\chi^2/\nu = 0.31$. We have tested the normality of residuals, and we find that they very likely correspond to a Gaussian distribution. This indicates that the experimental errors should probably be rescaled the by a factor less than $1/2$, i.e., the fit would be acceptable if the errors were twice smaller than stated in the experiment. This observation concerns all previous determinations of the dipolar axial mass from these neutrino data, based on fits trying to minimize the discrepancies with the experiment.

In Fig. 5 we plot the χ^2/ν values as a function of the two axial masses, showing that they are highly correlated. While the dipole form factor (two equal axial masses) is contained in the confidence region around the minimum, it is not the only allowed solution as two different axial masses also provide acceptable fits.

In order to study the sensibility of the results against general variations of the form factor, we also show in fig. 5 the χ^2/ν contour plots for the errors in the axial form factor $\delta G_A(Q^2)$ when the Q^2 values are binned with $\Delta Q^2 = 0.1 \text{ GeV}^2$ in the range $|Q^2| \leq 2 \text{ GeV}^2$. The χ^2 for each value of δG_A in a Q^2 bin has been computed by adding the specified value of δG_A to the form factor at the Q^2 values of the corresponding bin only. This shows that the value of χ^2 can be lowered further for more general variations of the axial form factor. To explore this issue deeper we have performed simultaneous variations of $\delta G_A(Q^2)$ in twenty Q^2 bins. A new minimum was found giving $\chi^2 = 23.8$ and $\chi^2/\nu = 0.17$. As seen in fig. 5 —and verified by our minimization— the data seems to favor a larger form factor around $|Q^2| = 0.4 \text{ GeV}^2$ and a smaller one around $1.2 - 2 \text{ GeV}^2$.

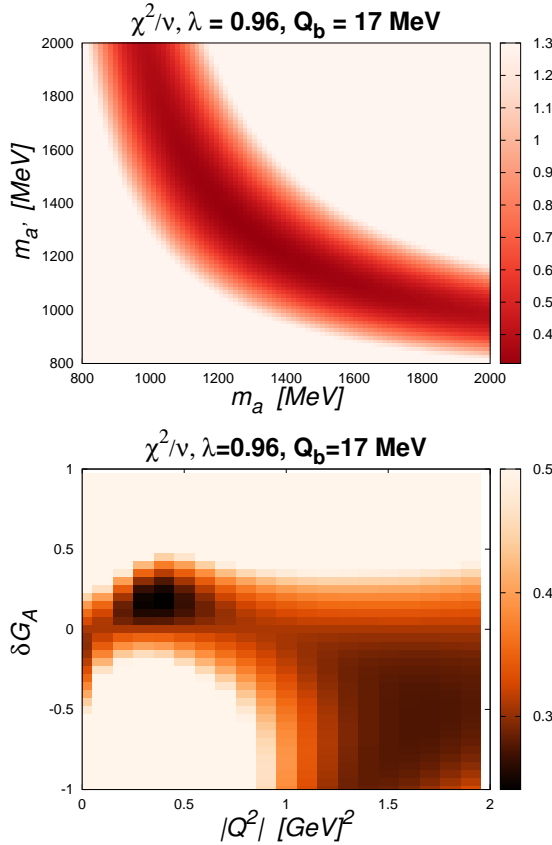


Figure 5: Top panel: χ^2 contour plot for the fitted axial masses. Bottom panel: χ^2 contour plots for the errors in the axial form factor $\delta G_A(Q^2)$ when the Q^2 values are binned with $\Delta Q^2 = 0.1 \text{ GeV}^2$ in the range $0.1 \text{ GeV}^2 \leq Q^2 \leq 2 \text{ GeV}^2$.

6. Conclusions and outlook

Most of the previous analyzes of the axial form factor based on MiniBonne neutrino data and a dipolar form suggest an unprecedented accurate but incompatible determination of this otherwise elusive quantity, regardless of the assumed nuclear model. We take here a different perspective. We assume a theoretically based axial form factor with an a priori uncertainty estimate, regardless of the neutrino data. Most remarkably the errors in the axial form factor determined by the axial-vector dominance using the half width rule, while quite generous, do not generally produce larger uncertainties than the experimental differential cross sections reported by the MiniBoone collaboration.

Acknowledgements

We thank Pere Masjuan for collaboration in the very early stages of this work. This work is supported by Spanish DGI (grant FIS2014-59386-P) and Junta de Andalucía (grant FQM225).

References

[1] A. Aguilar-Arevalo *et al.* (MiniBooNE Collaboration), *Phys. Rev. Lett.* **100**, 032301 (2008).

[2] A. Aguilar-Arevalo *et al.* (MiniBooNE Collaboration), *Phys. Rev. D* **81**, 092005 (2010).
[3] A. Aguilar-Arevalo *et al.* (MiniBooNE Collaboration), *Phys. Rev. D* **88**, 032001 (2013).
[4] H. Gallagher, G. Garvey, G.P. Zeller, *Annu. Rev. Nucl. Part. Sci.* **61**, 355 (2011).
[5] J.A. Formaggio, G.P. Zeller, *Rev. Mod. Phys.* **84**, 1307 (2012).
[6] J.G. Morfin, J. Nieves, J.T. Sobczyk, *Adv. High Energy Phys.* **2012**, 934597 (2012).
[7] L. Alvarez-Ruso, Y. Hayato, and J. Nieves, *New Jou. Phys.* **16** (2014) 075015.
[8] J. Nieves, I. Ruiz Simo, M.J. Vicente Vacas, *Phys. Lett. B* **707** (2012) 72.
[9] A.V. Butkevich, D. Perevalov, *Phys. Rev. D* **89** (2014) 053014.
[10] V. Bernard, L. Elouadrhiri, and U.G. Meissner, *Jou. Phys. G: Nucl. Part. Phys.* **28** (2002) R1.
[11] M. Martini, M. Ericson, G. Chanfray, J. Marteau, *Phys. Rev. C* **81** (2010) 045502.
[12] J.E. Amaro, M.B. Barbaro, J.A. Caballero, T.W. Donnelly, C.F. Williamson, *Phys. Lett. B* **696** (2011) 151.
[13] G.D. Megias, J.E. Amaro, M.B. barbaro, J.A. Caballero, T.W. Donnelly, *Phys. Lett. B* **725** (2013) 170.
[14] J. E. Amaro, E. R. Arriola and I. R. Simo, arXiv:1505.05415 [nucl-th].
[15] C. Wilkinson [T2K Collaboration], *PoS Nufact* **2014**, 104 (2015).
[16] P. Masjuan, E. Ruiz-Arriola, W. Broniowski, *Phys. Rev. D* **87**, 014005 (2013).
[17] Carl E. Carlson and J. L. Poor. *Phys. Rev.*, D34:1478, 1986.
[18] Bhubanjyoti Bhattacharya, Richard J. Hill, and Gil Paz. *Phys. Rev.*, D84:073006, 2011.
[19] A. Bodek, S. Avvakumov, R. Bradford, and Howard Scott Budd. *Eur. Phys. J.*, C53:349–354, 2008.
[20] K. F. Liu, S. J. Dong, Terrence Draper, J. M. Wu, and W. Wilcox. *Phys. Rev.*, D49:4755–4761, 1994.
[21] S. Capitani *et al.* *Nucl. Phys. Proc. Suppl.*, 73:294–296, 1999.
[22] C. Alexandrou *et al.* *Phys. Rev.*, D83:045010, 2011.
[23] Parikshit M. Junnarkar, S. Capitani, D. Djukanovic, G. von Hippel, J. Hua, B. Jger, H. B. Meyer, T. D. Rae, and H. Wittig. *PoS, LATTICE2014*:150, 2015.
[24] V. M. Braun, A. Lenz, and M. Wittmann. *Phys. Rev.*, D73:094019, 2006.
[25] Zhi-Gang Wang, Shao-Long Wan, and Wei-Min Yang. *Eur. Phys. J.*, C47:375–384, 2006.
[26] Guray Erkol and Altug Ozpineci. *Phys. Rev.*, D83:114022, 2011.
[27] T. D. Lee, S. Weinberg, and B. Zumino. *Phys. Rev. Lett.*, 18:1029–1032, 1967.
[28] T. D. Lee and B. Zumino. *Phys. Rev.*, 163:1667–1681, 1967.
[29] P. H. Frampton. *Phys. Rev.*, D1:3141–3151, 1970.
[30] M. Gari and U. Kaulfuss. *Phys. Lett.*, B138:29–31, 1984.
[31] Gerard 't Hooft. *Nucl. Phys.*, B72:461, 1974.
[32] Edward Witten. *Nucl. Phys.*, B160:57, 1979.
[33] P. Masjuan, E. Ruiz Arriola, and W. Broniowski. *Phys. Rev.*, D85:094006, 2012.
[34] C. A. Dominguez, *Riv. Nuovo Cim.* **8N6**, 1 (1985).
[35] J. Beringer *et al.* *Phys. Rev.*, D86:010001, 2012.
[36] J.E. Amaro, M.B. Barbaro, J.A. Caballero, T.W. Donnelly A. Molinari, and I. Sick, *Phys. Rev. C* **71**, 015501 (2005).
[37] J.E. Amaro, M.B. Barbaro, J.A. Caballero, T.W. Donnelly, C. Maieron, *Phys. Rev. C* **71**, 065501 (2005).
[38] J.E. Amaro, M. B. Barbaro, J. A. Caballero, and T. W. Donnelly. *Phys. Rev. Lett.*, 98:242501, 2007.